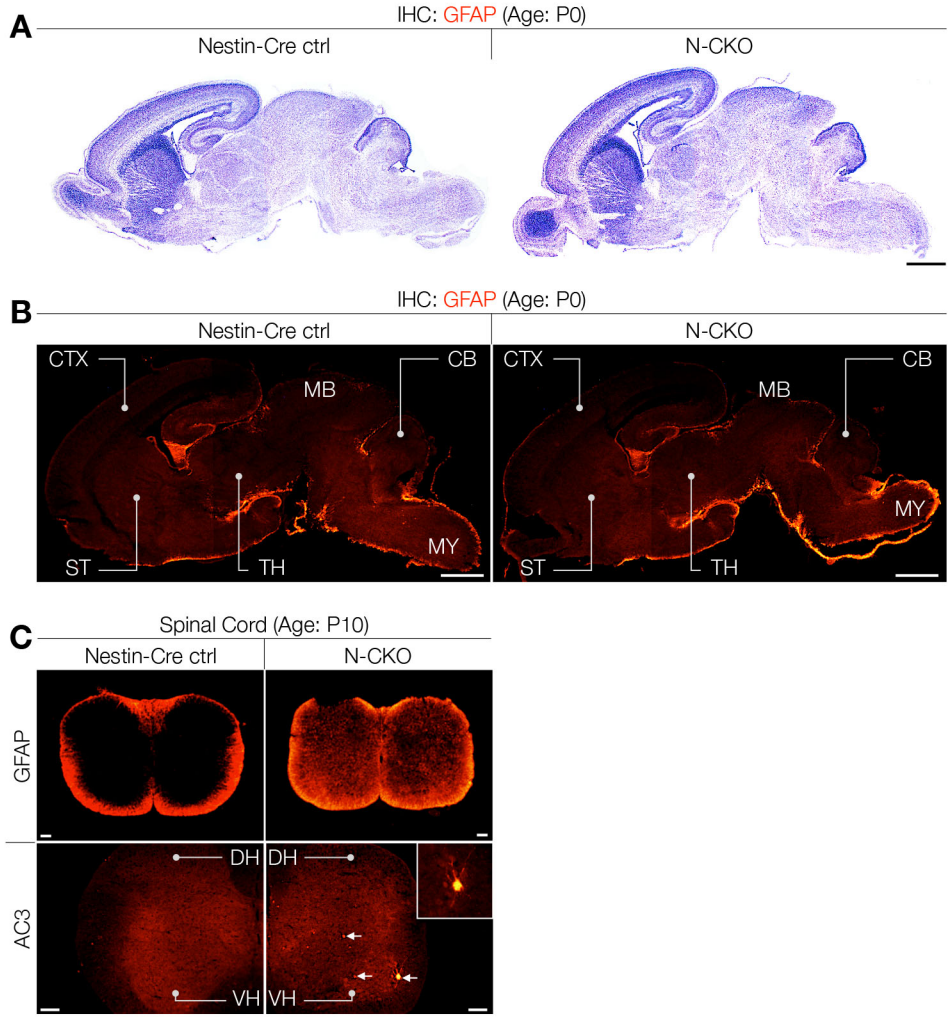


**Figure S1** Absence of histopathology in P0 N-CKO tissue. (**A**) Nissl stain of P0 N-CKO brain. Scale bar= 1 mm. (**B**) GFAP immunostaining. Scale bar= 1 mm. (**C**) GFAP and AC3 immunoreactivity in P10 spinal cords. N-CKO spinal cord exhibits gliosis and apoptosis. Arrows highlight activated caspase-3-positive nuclei in ventral horn (VH). DH: dorsal horn; VH: ventral horn. Scale bar= 100 $\mu$m.

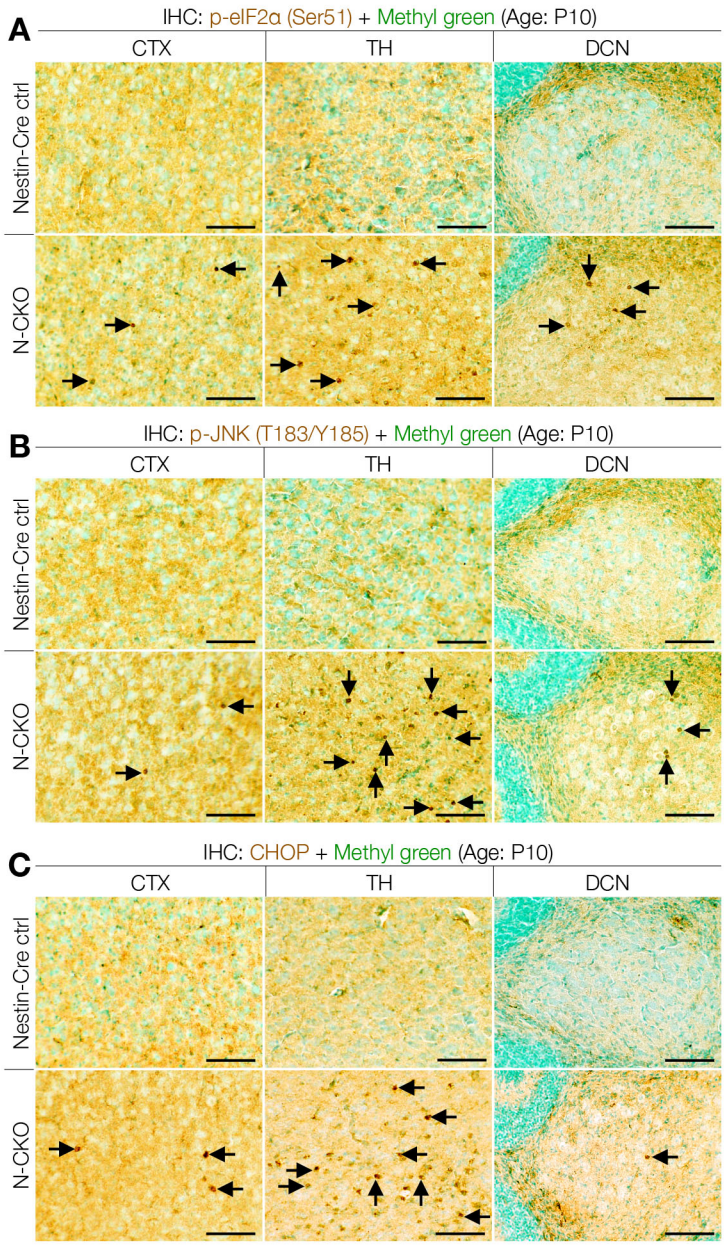


**Figure S2** N-CKO CNS tissue exhibits markers of ER-stress in susceptible sensorimotor regions. Immunostaining for (**A**) phospho-eIF2α (Ser51), (**B**) phospho-JNK (T183/Y185), and (**C**) nuclear-translocated CHOP is increased in vulnerable regions of N-CKO brains. Arrows highlight positive cells. Scare bar= 100 $\mu$m.

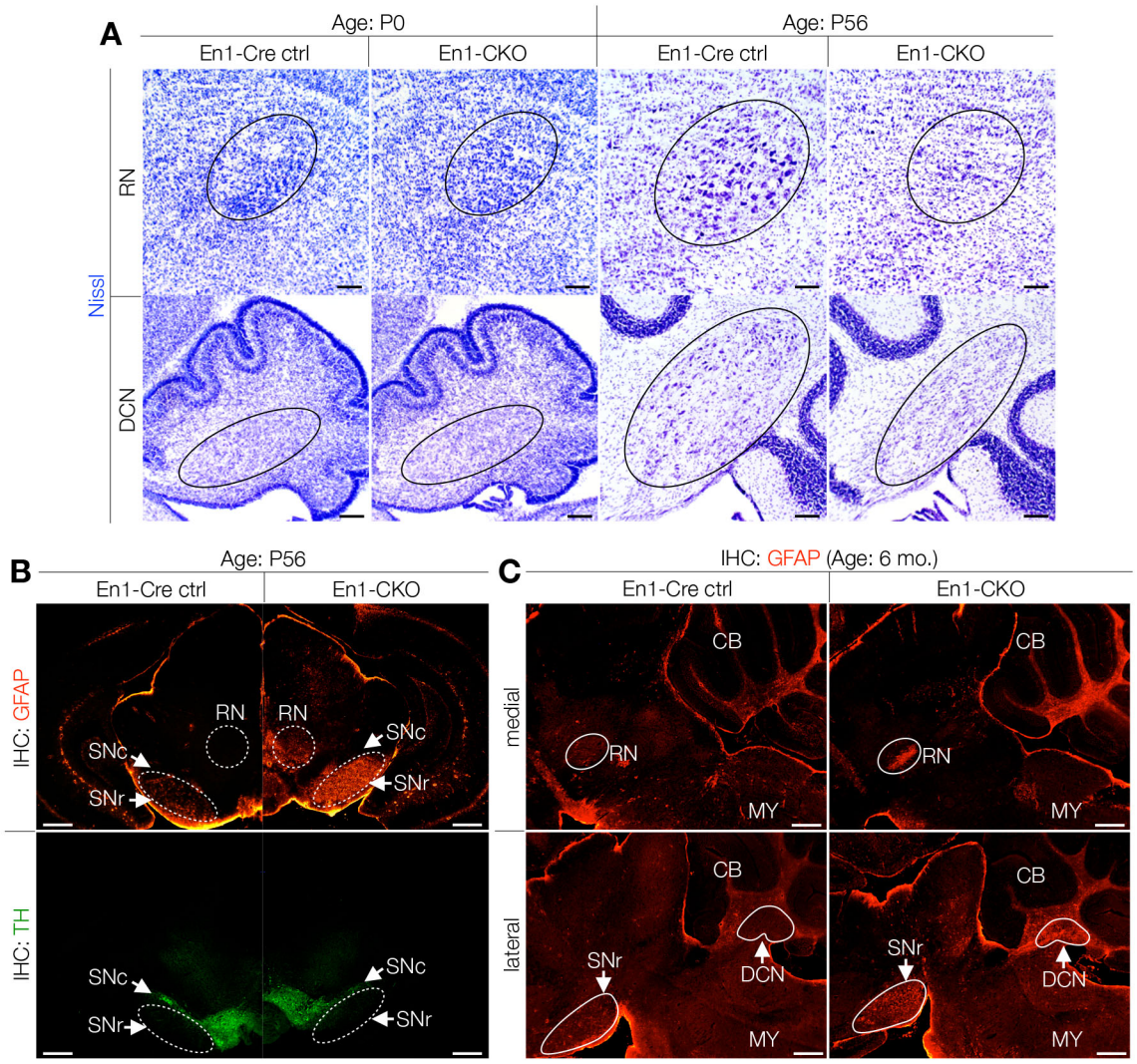


**Figure S3** Neurodegeneration in En1-CKO mutants. (**A**) Nissl staining of En1-CKO and control brain sections. En1-CKO brains appear normal at P0 but show profound neuronal loss in RN and DCN at P56. Scale bar= 100 $\mu$m. (**B**) GFAP and tyrosine hydroxylase (TH) immunostaining (P56). Gliosis is present selectively in RN and SNr of En1-CKO. SNc: substantia nigra pars compacta. Scale bar = 500 $\mu$m. (**D**) GFAP Immunoreactivity in 6-month En1-CKO and control brain sections. Gliosis remains confined tp RN, SNr, and DCN, with no spread to other Cre-expressing structures. Scale bar= 100 $\mu$m.

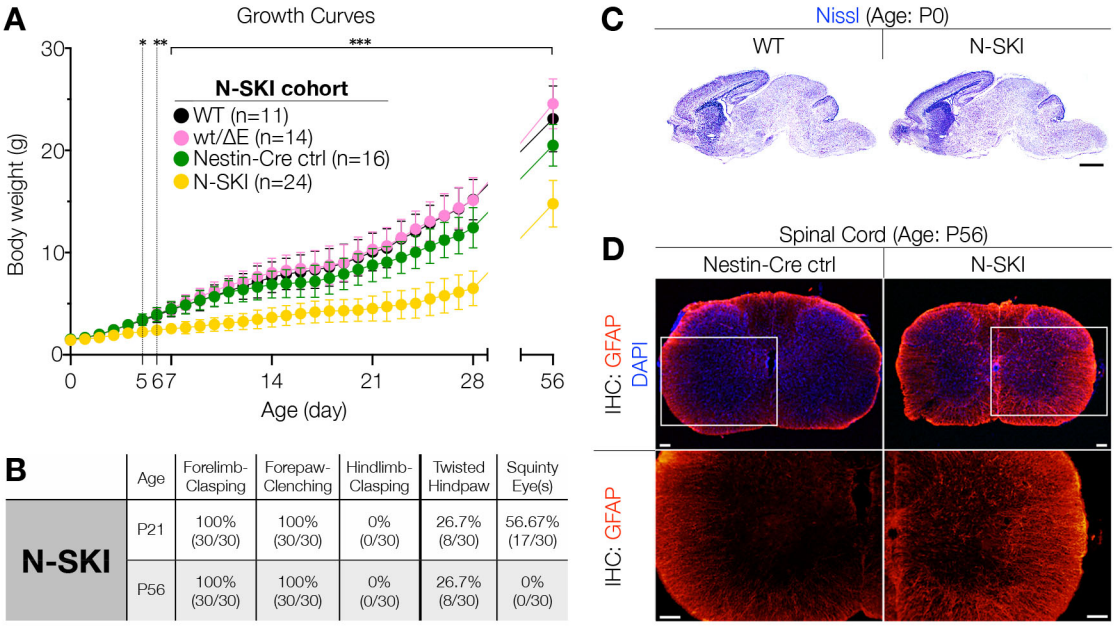


| | Age | Forelimb-Clasping | Forepaw-Clenching | Hindlimb-Clasping | Twisted Hindpaw | Squinty Eye(s) |
|---|---|---|---|---|---|---|
| **N-SKI** | P21 | 100% (30/30) | 100% (30/30) | 0% (0/30) | 26.7% (8/30) | 56.67% (17/30) |
| | P56 | 100% (30/30) | 100% (30/30) | 0% (0/30) | 26.7% (8/30) | 0% (0/30) |

**Figure S4** Characterization of N-SKI mice. (**A**) Growth curves. N-SKI mice become significantly lighter from P5 onward. 2-Way Anova, Mean (SD), *P<0.05; **P<0.01; ***P<0.001. (**B**) The frequency of N-SKI mutants showing various behavioral abnormalities at P21 and P56. (**C**) Nissl staining of N-SKI and control brains (P0). Scale bar= 1 mm. (**D**) GFAP immunoreactivity in N-SKI and control P56 spinal cords. Mild gliosis is present N-SKI tissue. Scale bar= 100 $\mu$m.

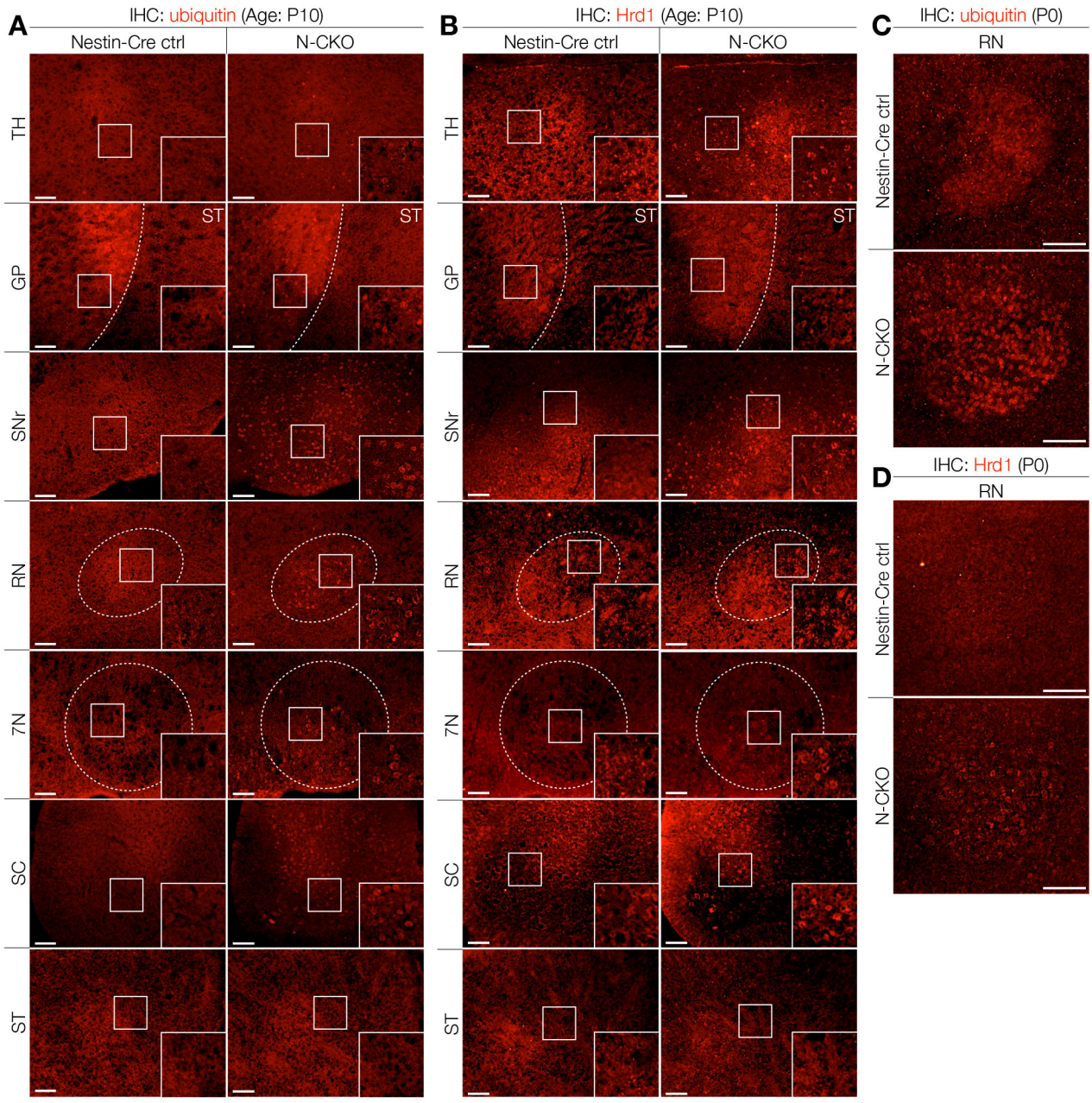


**Figure S5** Region selective abnormalities of ubiquitin and Hrd1 in N-CKO mice. For both molecules, the lack of abnormality in striatum illustrates that these molecular abnormalities are isolated to the structures exhibiting gliosis and neurodegeneration (**A**) Perinuclear accumulation of ubiquitin immunoreactivity (P10). Scale bar= 100 $\mu$m. (**B**) Perinuclear accumulation of Hrd1 immunoreactivity (P10). Scale bar= 100 $\mu$m. Abnormal perinuclear accumulation of ubiquitin (**C**) and Hrd1 (**D**) can be detected in RN of N-CKO as early as at P0. Scale bar= 100 $\mu$m.

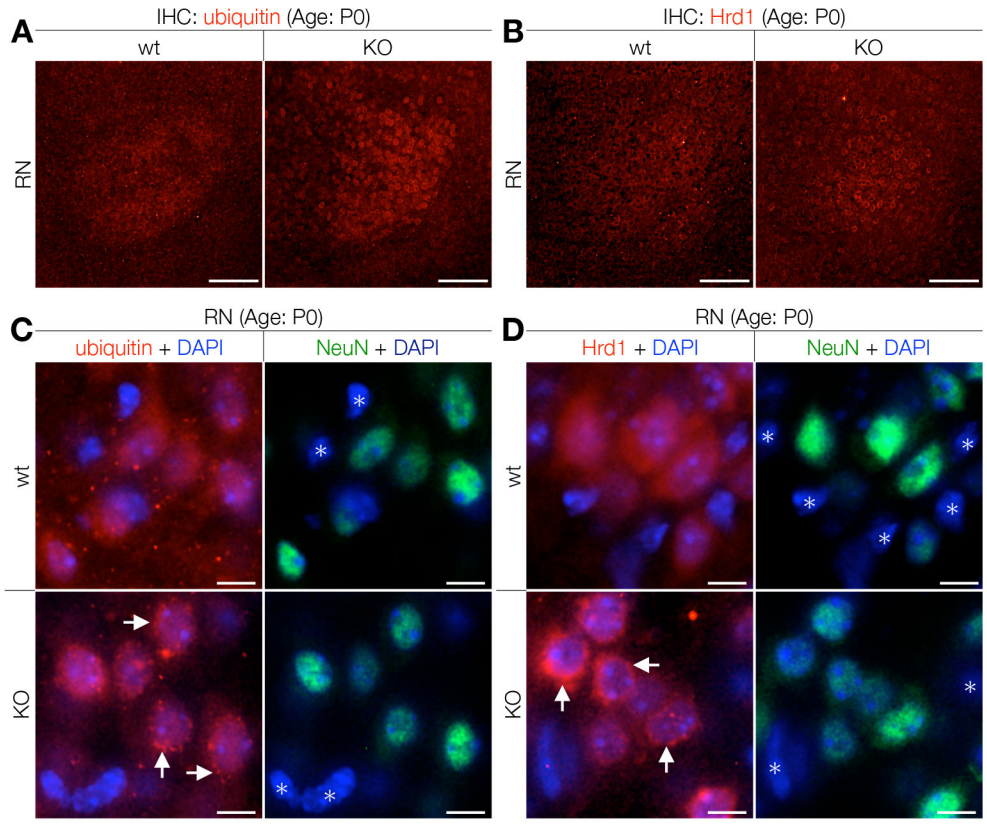


**Figure S6** Abnormal perinuclear accumulation of ubiquitin (**A**) and mislocalization of Hrd1 (**B**) in the RN of torsinA constitutive knockout (KO) at P0. Scale bar= 100 $\mu$m. (**C**) Only NeuN-positive cells in RN of torsinA-null mice (KO) show perinuclear ubiquitin-accumulation. Asterisks mark non-neuronal cells. Scale bar= 100 $\mu$m. (**D**) Hrd1 expression is neuron-specific and only NeuN-positive cells in RN of KO show abnormal Hrd1 mislocalization. Asterisks mark non-neuronal cells. Scale bar= 10 $\mu$m.

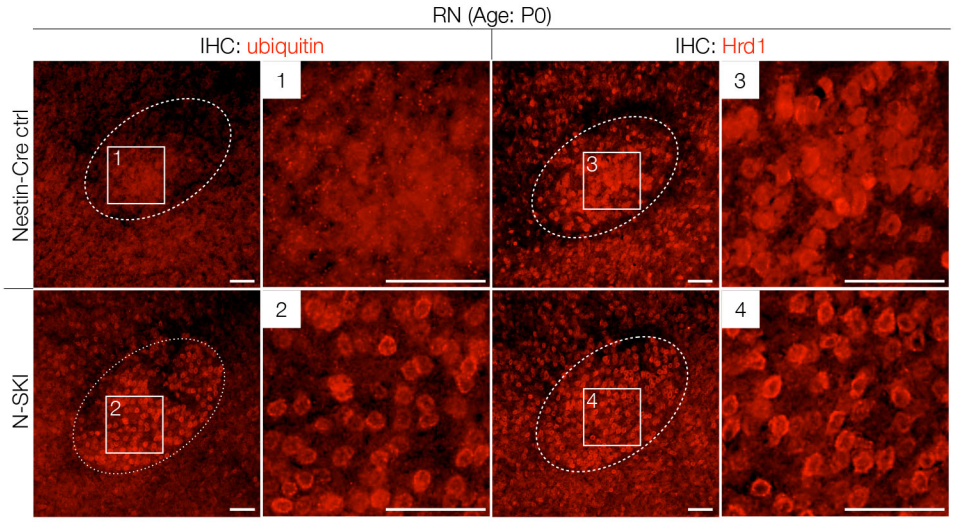


**Figure S7** Region selective abnormalities of ubiquitin and Hrd1 in N-SKI mice. Immunohistochemistry of ubiquitin and Hrd1 in P0 RN. Abnormal perinuclear ubiquitin accumulation and Hrd1 mislocalization show in RN of N-SKI at P0. Scale bar= 100 $\mu$m.